Bulgarian Chemical Communications, Volume 47, Number 1 (pp. 368–377) 2015

Intensity and SAR dependent changes in conformation of frog skeletal muscle total protein content after irradiation with 2.45 GHz electromagnetic field

T. I. Apostolova*

Department of excitable structures, Institute of Biophysics and Biomedical engineering, Bulgarian Academy of Sciences, Sofia, Bulgaria

Received December, 2014; Revised January, 2015

A study of the influence of 2.45 GHz electromagnetic field with high (20 mW/cm^2) and low (10 mW/cm^2) intensities on frog skeletal muscle protein conformation was engaged. Two different fractions (centrifuged at 900 g and 9600 g respectively) were preliminary exposed with the electromagnetic field and others were sham exposed. The same ones were lyophilized after that and processed with Fourier transform infrared spectroscopy using Bruker IFS 113 v. Specific absorption rate was calculated for both fractions and field intensities. The water mask was removed mathematically. The characteristic peaks and shoulders from Amid I and Amid II bands (descriptive for protein secondary structures) were decomposed and the area under them was calculated. The percentage decrease of α-helices after irradiation with the two intensity fields and in both fractions was observed. The changes of β-sheets, parallel β-structures, turns, bends and random coils were intensity and specific absorption rate dependent. Because of the temperature controlled conditions during the whole time of irradiation, we argue that these conformational changes are specific, non-thermal.

Key words: electromagnetic field, protein conformation, infrared spectroscopy, frog skeletal muscle.

INTRODUCTION

The investigations of microwave electromagnetic fields (EMF) and their influence on different biological structures exponentially increased during the last 30 years. This fact is due to the increased use and hence increasing exposure of different human groups. At the same time, the therapeutic use of EMFs in medical practice has increased markedly.

The cellular and sub-cellular mechanisms of the EMF effects are not yet well understood. There are different hypothesis and model investigations, but still there is no agreement achieved about the common mechanisms of EMF action on biological systems. The effects of microwaves (MMW) are usually classified as thermal (heat-producing) and non-thermal (specific, below the thermal noise at physiological temperatures). Many authors accept that the effects of MMW are due only to the temperature rising in the irradiated object [1–9]. In the case of large molecules the energy shares out in the whole molecule and not enough quantity remains to cause covalent bonds breaking. The energy is taking out from the system with oscillating atoms and converts to heat. In the biological systems the absorbed microwave energy transforms to the increasing kinetic energy, which in that way causes common heating of the different tissues. This heating is a result from ion conductance and vibration of dipole water molecules and peptides [10, 11]. The MMW absorption depends on the medium electrical properties – dielectric constant, electrical conductance and hence wave penetration depth. These properties are changing with EMF frequency [12]. On the basis of these properties one can define the depth of penetration of the EMF of particular frequency. In tissues with low water content (like adipose tissue) the penetration of EMF is vastly higher than in these with high water content (like muscle tissue). At the same time the depth of penetration decreases with frequency growth.

The interaction between MMW and living creatures depends on characteristics like field oscillation frequency and field intensity. Relative boundary between low- and high-intensity EMF is accepted to

* To whom all correspondence should be sent:
E-mail: tivukova@bio.bas.bg

be 10 mW/cm^2 [13]. At sub-cellular level the action of EMF is connected with dielectric properties of biomacromolecules and macromolecule aggregates, as enzyme complexes, membrane receptors and ion channels [14]. If one applies conventional heating, the kinetic energy is introduced in all molecules, while after EMF irradiation the influence is on polarized and charged molecules, and ions. As the water molecules possess large polar moment they absorb the microwave energy with priority, and hence become more mobile and probably more reactive [15].

There are no controversial opinions observed concerning the nonspecific – temperature effects of MMWs up to this moment. With regard to the specific – non-temperature effects of MMWs consensus is not achieved presently. Despite all that, we can find out in literature the increasingly experimental and model data about these effects. Recently published experimental data argues about specific effect on protein conformation of EMF field with frequency 1765 MHz and 800 mW/m^2 power density on myoglobin structure through increasing of β-sheet content with respect to α-helix content decreasing [16]. The same authors [17] observed similar effects on bovine ground meet after irradiation with 2.45 GHz MMW.

We were inspired by these data to further investigate whether there is any specific (non-thermal) effect of 2.45 GHz electromagnetic field with low (10 mW/cm^2) and high (20 mW/cm^2) power densities on compound protein, derived from frog skeletal muscle.

EXPERIMENTAL

Object and methods of investigation

Striated muscles from summer and autumn frogs (*Rana ridibunda*) was homogenized with 0.5 M Na/P buffer pH 7.6 for 1 minute. The homogenate was centrifuged after that for 15 minutes at 900 g (3600 ob. /min) at 4^o C. The supernatant was centrifuged after that for 30 min at 9600 g (12000 ob./min). At this stage nuclei and mitochondria were removed. The obtained fractions were divided into two equal quantities of a 15 ml and were placed in two Petri dishes with 96 mm diameter, making thin films of a 2 mm on the bottom of the dishes. The Petri dishes after that were placed at 25 °C temperature. One of the dishes was irradiated for 30 min with 2.45 GHz electromagnetic field (10 and 20 mW/cm^2 power density), whereas the other was sham exposed at this time. Two probes were placed on ice in order to maintain constant temperature. At the end of irradiation the temperature changes were between 1.8–2 °C.

The fractions were then lyophilized with USIFROID SMH50 for 44 hrs. at a temperature 45 °C and 180 μBar pressure. The lyophilized probes were analyzed by Fourier transform infrared spectroscopy (FTIRS) in order to analyze the conformational changes of compound proteins in lyophilized probes. FTIRS was made at three reiterations in KBr tablets in absorption interval of 1800–1400 cm^{-1} with accuracy 0.1–0.2 cm^{-1} on Bruker IFS 113 V apparatus.

Computation and statistical analysis

Structural information and quantity information about the protein secondary structures is obtained by decomposition of Amid I and Amid II bands at the interval of 1800–1400 cm^{-1} using the method of Arrondo et al. [18, 19]. The procedure is based on deconvolution of the curve of infrared spectre and its compounds in boundaries of Amid I and Amid II bonds. The first step is evaluation of the characteristic shoulders and peaks and rough assessment of their shape (width and height). This operation is necessary for the start of the iterative procedure with Gaussian functions. After this operation the area under the peaks and shoulders is determined. The information from Amid I (1600–1700 cm^{-1}) band is due to vibrational stretching of C=O peptide groups (nearly 80%), whereas the Amid II band (1510–1580 cm^{-1}) is characteristic for β-sheets movement. The calculation procedure was made by MATLAB package.

The data for the secondary structures were presented as mean values ± standard deviation (SD). One-way ANOVA was used to evaluate the statistically significant differences between exposed and sham exposed groups with high- and low-intensity fields (with 20 and 10 mW/cm^2 intensities respectively). In all four groups of experiments the number of reiterations were eight (n=8) in order to achieve Gaussian distribution.

The specific absorption rate (SAR) calculation

The magnetic permeability of most tissues is practically equal to that of free space, and all known and anticipated interactions at higher radio frequencies occur through mechanisms involving the electrical (E) field (including the currents induced by the magnetic (H) field). Therefore, the E-field vector, or its distribution throughout the exposed object, fully describes the exposure field-tissue interactions. A dosimetric measure that has been widely adopted is the specific absorption rate (SAR) defined as "the time derivative of the incremental energy absorbed by, or dissipated in an incremental mass contained in a volume element of a given density" and is cal-

culated using the Poynting vector theorem for sinusoidal varying electromagnetic fields [20].

The model of SAR calculation was based on the assessment of the energy across a plane section of the flux, formed by a cone with a vertex in the amplitude centre. Homogenous electrical field represented the flux in the cone. The average SAR, defined as a ratio between the total energy absorbed in the exposed object (E_l) and its mass (m_l), is:

$$SAR = \frac{E_l}{m_l}$$

The energy was defined from the densities of the electric components of the generated electromagnetic field and the characteristic parameters of the exposed object. The average SAR was calculated according to the mathematical model described earlier [21]. SAR values for the fraction centrifuged at 900 g was: for low intensity field (10 mW/cm^2) – 4.92 mW/mg; for high intensity field (20 mW/cm^2) – 9.83 mW/mg. SAR values for the fraction centrifuged at 9600 g was 5.08 mW/mg and 10.2 mW/mg respectively.

RESULTS

Changes of secondary structures in membrane fraction centrifuged at 900 g after irradiation

The Amid I band is localised between 1600 cm^{-1} and 1800 cm^{-1} and Amid II band is localised between 1510 cm^{-1} and 1580 cm^{-1}. The peaks and shoulders content is characteristic for the secondary protein conformation.

The data from FTRIS show changes of the absorption maximum compared to the control at 1653 cm^{-1} in all groups observed. Additional absorption peaks were observed at 1695 cm^{-1}, 1683 cm^{-1}, 1645 cm^{-1} and 1635 cm^{-1}, as well as weak shoulders at 1657 cm^{-1} and 1617 cm^{-1} (Figs 1 and 2). The maximum of the peak in Amid II band is at 1599 cm^{-1} with additional absorption peaks at 1576 cm^{-1}, 1559 cm^{-1}, 1719 cm^{-1}, and 1507 cm^{-1} and a shoulder at 1521 cm^{-1} (Figs 1 and 2 down curves). Out of the characteristic Amid I and Amid II curves was observed one more characteristic peak at 1733 cm^{-1} which depicts weak lipid-protein interactions.

After irradiation with low-intensity field (10 mW/cm^2) (Fig. 1 upper curve) the maximum in Amid I band is once again at 1653 cm^{-1}, but there are additional shoulders at 1695 cm^{-1} and 1657 cm^{-1}. In Amid II band the peak at 1549 cm^{-1} is shifted at 1547 cm^{-1} with additional absorptions at 1576 cm^{-1}, 1540 cm^{-1} and 1505 cm^{-1}.

The irradiation of probes with high intensity EMF (20 mW/cm^2) (Fig. 2, down curve) the absorption peaks of Amid I band are at 1695 cm^{-1}, 1685 cm^{-1}, 1643 cm^{-1}, 1635 cm^{-1}, 1617 cm^{-1} and 1602 cm^{-1} with maximum peak at 1653 cm^{-1}. In Amid II band the maximums are at 1559 cm^{-1} and 1540 cm^{-1}, with additional absorption shoulders at 1576 cm^{-1}, 1571 cm^{-1}, 1554 cm^{-1}, 1547 cm^{-1}, 1521 cm^{-1}, and 1508 cm^{-1}.

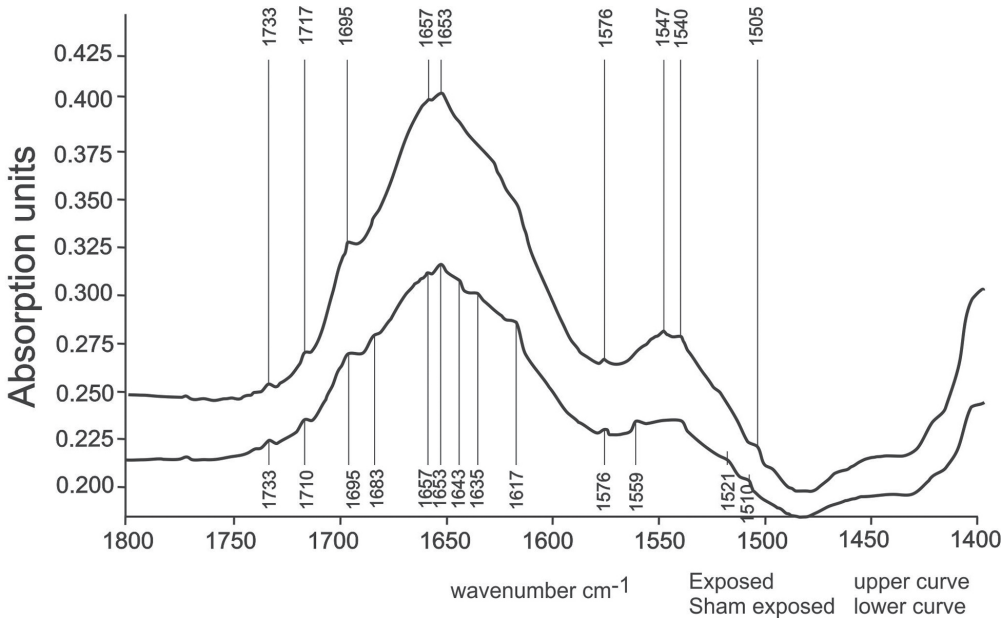

Fig. 1. Example of infrared spectra from sham exposed (lower curve) lyophilised homogenates of frog skeletal muscle, centrifuged at 900 g, and from exposed ones (upper curve) with low intensity field (10 mW/cm^2)

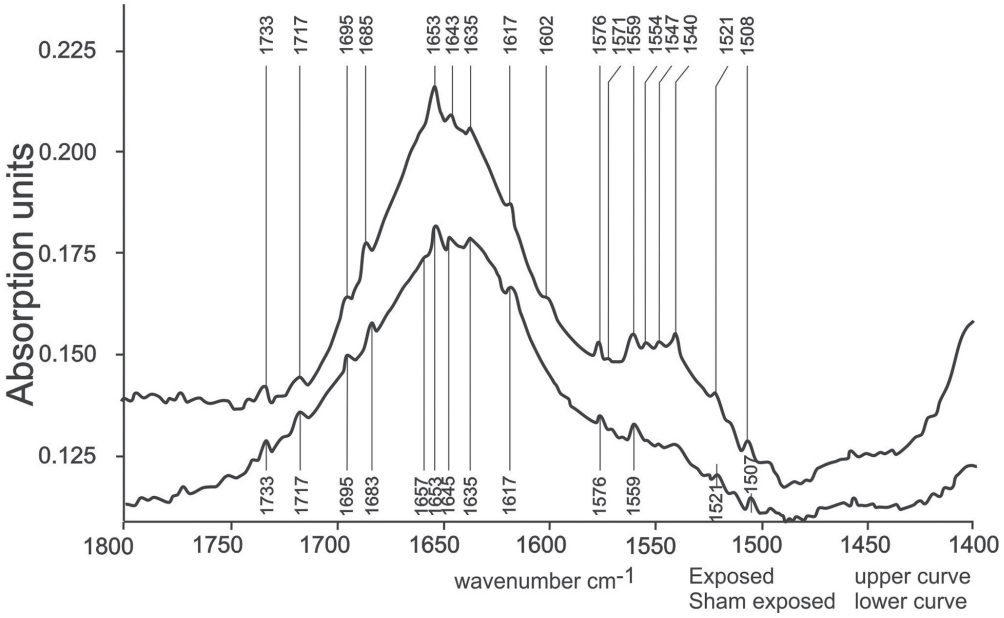

Fig. 2. Example of infrared spectra from sham exposed (lower curve) lyophilised homogenates of frog skeletal muscle, centrifuged at 900 g, and from exposed ones (upper curve) with high intensity field (20 mW/cm^2)

The percentage changes of the basic secondary structures of low intensity (Table 1) and high intensity-field was calculated (Table 2) on the basis of these characteristic peaks and shoulders. I observed statistical significant changes of α-helices after irradiation with both intensities (Table 1 and 2). The low intensity field influenced statistically significant unordered structures (turns, bends and coils) (Table 1). The high intensity field caused statistically significant lowering of parallel β-structures, as well as statistically significant increasing of unordered structures (Table 2).

Table 1. Quantification of secondary peptide structure derived from peaks and shoulders obtained from FTIRS of sham exposed and exposed with low intensity field (10 mW/cm^2) homogenates of frog skeletal muscle, centrifuged at 900 g (first column). Second column – the quantity in percentage of corresponding peaks and shoulders

Sham exposed		Exposed	
(1)	(2)	(1)	(2)
α-helices 1653 cm^{-1} 1557 cm^{-1}	Total 38%±3.9%	α-helices 1653 cm^{-1} 1557 cm^{-1}	Total 29%±3.6%*
β-sheets 1695 cm^{-1} 1683 cm^{-1} 1617 cm^{-1} 1576 cm^{-1}	Total 22 %±1.8%	β-sheets 1695 cm^{-1} 1683 cm^{-1} 1617 cm^{-1} 1576 cm^{-1}	Total 23%±2.54%
parallel β-structures 1643 cm^{-1} 1635 cm^{-1}	Total 10%±1.13%	parallel β-structures 1643 cm^{-1} 1635 cm^{-1}	Total 9%±1.73%
Turns, bends and random coils 1626 cm^{-1} 1521 cm^{-1}	Total 30%±3.5%	Turns, bends and random coils 1626 cm^{-1} 1521 cm^{-1} 1505 cm^{-1}	Total 39%±2.28%*

Table 2. Quantification of secondary peptide structure derived from peaks and shoulders obtained from FTIRS of sham exposed and exposed with high intensity field (20 mW/cm^2) homogenates of frog skeletal muscle, centrifuged at 900 g (first column). Second column – the quantity in percentage of corresponding peaks and shoulders

Sham exposed		Exposed	
(1)	(2)	(1)	(2)
α-helices 1653 cm^{-1} 1559 cm^{-1}	Total 38%±2%	α-helices 1653 cm^{-1} 1559 cm^{-1}	Total 30%±2.91%*
β-sheets 1695 cm^{-1} 1683 cm^{-1} 1617 cm^{-1} 1507 cm^{-1}	Total 22 %±2.33%	β-sheets 1695 cm^{-1} 1683 →1685cm^{-1} 1617 cm^{-1} 1507→1508 cm^{-1}	Total 21 %±2.07%
parallel β-structures 1643 cm^{-1} 1635 cm^{-1}	Total 10%±1.6%	parallel β-structures 1643 cm^{-1} 1635 cm^{-1}	Total 35%±3.76%***
Turns, bends and random coils 1626 cm^{-1} 1521 cm^{-1}	Total 30%±2.56%	Turns, bends and random coils 1602 cm^{-1} 1521 cm^{-1}	Total 14%±1.03%***

Changes of secondary structures in fraction centrifuged at 9600 g

The absorptions of the probes irradiated with low- and high-intensity fields in comparison to their sham exposed controls are shown on Figs. 3 and 4. The data from sham exposed preparation showed main absorption maximum at 1653 cm^{-1} in Amid I band. Additional absorption peaks are observed at 1695 cm^{-1}, 1684 cm^{-1}, 1635 cm^{-1}, as well as weak shoulders at 1626 cm^{-1} and 1617 cm^{-1} (Figs 3 and 4, lower curves). For Amid II band the maximum is localised at 1558 cm^{-1} and there are additional absorption peaks at 1576 cm^{-1}, 1533 cm^{-1}, 1516 cm^{-1} and 1507 cm^{-1} with absorption shoulder at 1521 cm^{-1} (Figs 3 and 4, down curves).

After irradiation with both intensity fields, the maximums are shifted from 1653 cm^{-1} to 1657 cm^{-1}

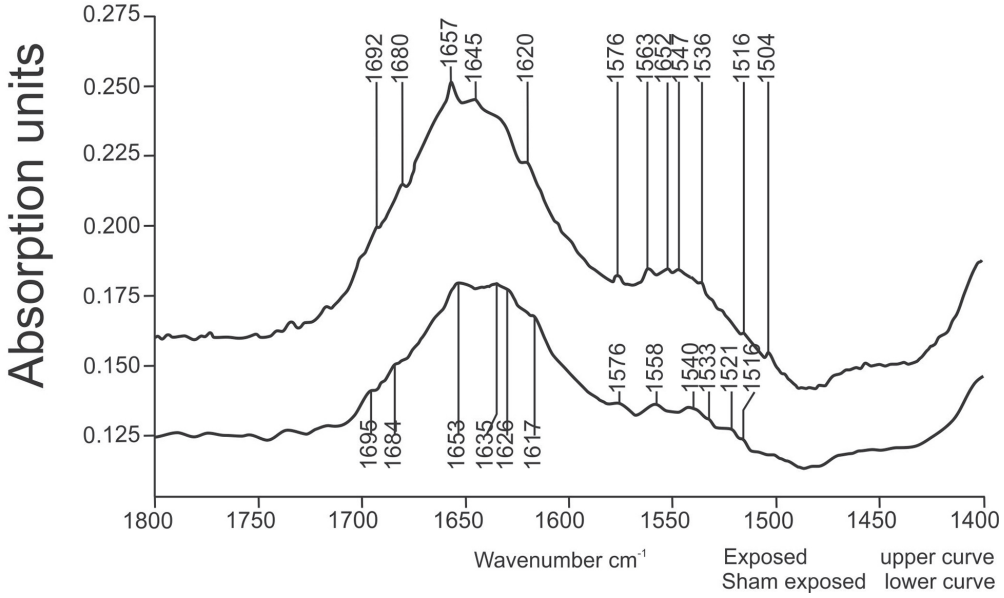

Fig. 3. Example of infrared spectra from sham exposed (lower curve) lyophilised homogenates of frog skeletal muscle, centrifuged at 9600 g, and from exposed ones (upper curve) with low intensity field (10 mW/cm^2)

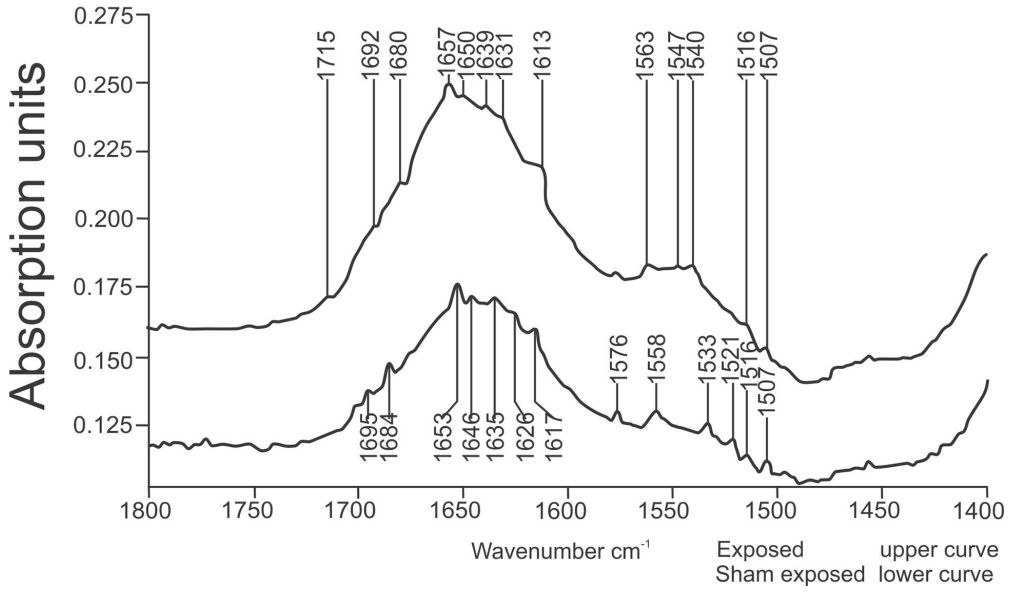

Fig. 4. Example of infrared spectra from sham exposed (lower curve) lyophilised homogenates of frog skeletal muscle, centrifuged at 9600 g, and from exposed ones (upper curve) with high intensity field (20 mW/cm^2)

Table 3. Quantification of secondary peptide structure derived from peaks and shoulders obtained from FTIRS of sham exposed and exposed with low intensity field (10 mW/cm^2) homogenates of frog skeletal muscle, centrifuged at 9600 g (first column). Second column – the quantity in percentage of corresponding peaks and shoulders

Sham exposed		Exposed	
(1)	(2)	(1)	(2)
α-helices 1653 cm^{-1} 1558 cm^{-1}	Total 31%±3.5%	α-helices 1653→1557 cm^{-1} 1558→1563 cm^{-1}	Total 16.14%±2.4%*
antiparallel β-forms 1695 cm^{-1} 1684 cm^{-1} 1617 cm^{-1} 1516 cm^{-1} 1507 cm^{-1}	Total 11.65%±2.4%	antiparallel β-forms 1695→1692 cm^{-1} 1684→1680 cm^{-1} 1617→1620 cm^{-1} 1516 cm^{-1} 1507→1504 cm^{-1}	Total 41.21%±1.52%
parallel β-forms 1646 cm^{-1} 1635 cm^{-1}	Total 23.22%±1.4%	parallel β-forms 1645 cm^{-1} 1635 cm^{-1}	Total 14.1%±3.4%
turns, coils, bends 1626 cm^{-1} 1521 cm^{-1}	Total 14.6%±1.7%	turns, coils, bends 1626 cm^{-1} 1521 cm^{-1} 1504 cm^{-1}	Total 48.1%±1.6%*

and additional peaks at 1680 cm^{-1} and 1692 cm^{-1} are observed. The irradiation with low-intensity field caused the appearance of two additional shoulders at 1645 cm^{-1} and 1620 cm^{-1}. Additional shoulders after high intensity field irradiation are observed at 1650 cm^{-1}, 1639 cm^{-1}, 1631 cm^{-1} and 1613 cm^{-1} (Figs 3 and 4). There was observed additional shoulder out of Amid I and Amid II ranges at 1715 cm^{-1} after irradiation with 20 mW/cm^2 field (Fig. 4, down curve).

In Amid II band the maximum was shifted from 1558 cm^{-1} to 1563 cm^{-1} after irradiation with both

Table 4. Quantification of secondary peptide structure derived from peaks and shoulders obtained from FTIRS of sham exposed and exposed with high intensity field (20 mW/cm^2) homogenates of frog skeletal muscle, centrifuged at 9600 g (first column). Second column – the quantity in percentage of corresponding peaks and shoulders

Sham exposed		Exposed	
(1)	(2)	(1)	(2)
α-helices 1653 cm^{-1} 1558 cm^{-1}	Total 33.3%±2.6%	α-helices 1653→1557 cm^{-1} 1558→1563 cm^{-1}	Total 15.26%±2.2%**
antiparallel β-forms 1695 cm^{-1} 1684 cm^{-1} 1617 cm^{-1} 1516 cm^{-1} 1507 cm^{-1}	Total 8.43%±1.73%	antiparallel β-forms 1695→1692 cm^{-1} 1684 →1680cm^{-1} 1617→1613 cm^{-1} 1516 cm^{-1} 1507 cm^{-1}	Total 10.33%±1.69%*
parallel β-forms 1646 cm^{-1} 1635 cm^{-1}	Total 17.9%±1.3%	parallel β-forms 1646→1650 cm^{-1} 1635→1639 cm^{-1}	Total 20.6%±2%
turns, coils, bends 1626 cm^{-1} 1521 cm^{-1}	Total 40.37%±1.8%	turns, coils, bends 1626→1631 cm^{-1} 1521 cm^{-1}	Total 53.81%±1.75%**

fields. The low-intensity field provoked additional shoulders at 1552 cm^{-1}, 1547 cm^{-1}, 1536 cm^{-1} and 1504 cm^{-1} (Fig. 3, upper curve).

On the basis of peaks position changes and changes in the area under them, secondary structures alteration after the irradiation was calculated (Tables 3 and 4). After low intensity field exposure was observed statistically significant lowering of α-helices and structures (Table 3). After high-intensity field irradiation was observed statistically significant decreasing of α-helices and β-sheets, as well as a growth of percentage content of turns, bends and coils (Table 4).

DISCUSSION

A number of authors presumed that the EMF irradiation influences the activity of an exact protein through the influence of its conformation. The ability of microwave irradiation to cause changes in protein conformation is largely debated by several teams [22–27].

Böhr and Böhr [24, 25] suggested that after irradiation of protein molecule vibrational stations of little moving parts of the molecule decrease their vibrational frequency and increase their axis length respectively, which is in agreement with Fröhlich [28] hypothesis. They supposed that these preconditions may lead to conformational changes in these proteins and hence to different biological effects of EMF on certain structure. The authors observed conformational changes of different proteins in solution after irradiation with MMW with 2.45 GHz frequency and 800 W power density.

The effects of impulse EMF with very low densities on protein conformation were observed by Neshev and Kirilova, [29]. They assume that the cell reacts on irradiation by stress answer. This answer acts by Hsp-proteins and it is very important for the normal cell function. Hsp-proteins act as "molecule companions", which bind and stabilise damaged protein conformation. In that way they defend the cell from outward stress factors.

Laurence et al. [23] discuss the theoretical opportunity low intensity impulse EMFs to influence specifically protein conformation. They compare different characteristics of the fields and protein molecule interactions like irradiation time, characteristic time of protein cooling in water solution, characteristic time of energy diffusion in macromolecule vibrational regime, characteristic time of protein unfolding. In the light of these comparisons they conclude that EMF with low intensity (10 mW/cm^2) and of the order of GHz frequency theoretically influences protein conformation. The authors suggest that the mechanism of protein conformation changes is resonance absorption of the field energy with afterward energy diffusion in water surrounded, or vice versa. After irradiation with very low intensity fields, it is supposed that they resonance with a few amino acid groups in proteins, so they can change the action of the corresponding enzyme active centre [30]. This hypothesis can explain the observation of

the so called "intensity windows". Small conformational changes after exposure to low intensity EMFs can greatly affect protein functionality in comparison to those after exposure with high intensity field, where the functionality can be lost because of the appearance of stronger changes in protein conformation [21].

Conformational changes after irradiation presume functional alteration of membrane ion channels, receptors, enzymes (membrane bonded or free). Thompson et al. [32] hypothesised changes in Ca^{2+}-binding after irradiation. They assumed that conformational changes of Ca^{2+}-binding proteins are due to the increased amount of ordinary structures responsible for binding this ion. The authors suggest that this mechanism agrees with the postulate of the so called "intensity windows".

Batanov et al [33] observed increasing of α-helices in albumin after irradiation with MMW. At the same time they did not observe breaking polypeptide chains or protein oligomerization. Changes of albumin's secondary structure is linearly connected with the field power.

Protein molecules possess high surface potential energy and non-harmonic dynamics [34]. As it is considered that protein biological function is connected with non-harmonic dynamics, the mechanism of binding between protein motion and its function is on the basis of interaction between EMFs and these large molecules. This protein dynamics is based on the following: 1) Globular proteins have vigorously packed structures and their conformational changes require common motion of most of the protein atoms; 2) For a molecule to undergo a conformational change from one structure to another, general vibrational regimes must be excited to jump over the energy barrier.

In our previous study [35] decreasing of α-helices quantity and increasing of unordered structures and β-sheets as a whole was shown. As the shift of amino acid activity in catalytic centre is vulnerable in rate of angstroms in order to be functional in biological systems we can speculate that the appearance of "intensity windows" connected with MMW irradiation is far more common. An interesting point is that after irradiation with low intensity field the changes in secondary protein structures are more pronounced. I suppose that the influence is specific (non-temperature), because the experiments were carried out in controlled temperature conditions. This suggestion is in congruence with the hypothesis of Böhr and Böhr [24, 25] which postulate that after irradiation the vibrational modes of little particles of the protein molecule decrease their vibrational frequencies, and is also in agreement with Fröhlich's [36, 37] hypothesis that the energy of EMFs does not disseminate like heat, but is stored in vibrational modes of large protein molecules. I can infer that in my case after irradiation with 10 mW/cm^2 and 20 mW/cm^2 EMFs the energy was sufficient to arouse common vibrational modes of protein molecule in such a way as to nip over the energy barrier.

In our investigations the information from characteristic Amid I and II bands confirmed lowering of α-helices quantity in two fractions estimated, exposed with EMF with two power densities [35]. This phenomenon was more pronounced in "rough membrane fraction". This is in accordance with the presence of the so called "intensity windows" referred to by other authors. Additional absorption peak is observed in "rough membrane fraction" which is out of the two Amid bands at 1733 cm^{-1}. It is characteristic of lipid-peptide hydrophobic interactions. Interestingly, the samples irradiated with low intensity field exhibit relatively more pronounced changes of protein secondary structure. We propose that the effect is specific (non-temperature) due to controlled temperature conditions of the experiment. This is in accordance with Böhr and Böhr [24, 25] hypothesis which states that if a peptide molecule is irradiated with microwave EMF the vibrational modes of little moving parts decrease their vibrational frequency. Another hypothesis that matches well our findings states that the energy from EMF entered the cells does not transform in thermal energy but is stored in peptide molecules and macromolecule vibrational modes. We can assume that in our case the energy from exposure was sufficient to excite general vibrational modes of peptide molecules to a level suitable for jumping over the energy barrier, leading to observed conformational changes.

In conclusion the EMF irradiation with two intensities influences statistically significant protein conformation in the direction of diminishing of α-helices and increasing of β-sheets and unordinary structures. In fraction centrifuged at 900 g there were observed changes of hydrophobic lipid-peptide interactions.

Acknowledgement: *The author expresses his acknowledgement to Ilina Amer for her kind assistance in stylistically editing and formatting of this article, and to d-r Nikolina Radicheva for her methodological support.*

REFERENCES

1. M. Boon, L. P. Kok, Microwave cookbook of pathology. Coulomb Press Leyden, Leiden, The Netherlands, 1987.
2. E. Marani, P. Bolhuis, M. E. Boon, *Histochem. J.*, **20**, 658 (1988).
3. Z. Wang, R. Van Dorp, A. F. Weidema, D. L. Yepey, *Eur. J. Morphol.*, **29**(3), 198 (1991).

4. E. C. Pollard, *Amer. Sci*., **57**, 206 (1969).
5. C. K. Chou, H. Bassen, J. Osepchuk J, Q. Balzano, R. Petersen, M. Meltz, R. Cleveland, J. C. Lin, L. Heynick, (1998): *Bioelectromagnetics*, **17**(3), 195 (1998).
6. E. M. Czerska, E. C. Elson, C. C. Davis, M. L. Swicord, P. Czerski P, *Bioelectromagnetics*, **13**(4), 247 (1992).
7. L. P. Kok, M. E. Boon, Microwave cookbook for microscopists. Art and science of visualization, Coloumb press, Leyden, The Netherlands, 1992.
8. E. Marani, H. K. Feirabend, *Eur. J. Morphol.*, **32**(2–4), 330 (1994).
9. R. Van Dorp, E. Marani, M. E. Boon, *Methods*, **15**(2), 151 (1998).
10. C. C. Johnson, A. W. Gui, *Proc TEEE*, **60**, 692 (1972).
11. L. J. Challis, *Bioelectromagnetics Suppl*, **7**, S98 (2005).
12. H. P. Schwan, K. Li, *Proc. IRE*, **41**, 1735 (1953).
13. N. D. Devyatkov, O. V. Betskii eds., Biological aspects of low intensity millimeter fields, Moscow, 1994.
14. P. P. Bernardi, D'Inzeo, in: Electromagnetic bio-interaction: mechanisms, safety standarts, protection guide, Franceschettu G, Gandhi M, Gandolfo M (eds.), Plenum Press, New York, 1989, p. 27.
15. J. M. Ruijgrok, M. E. Boon, H. Feirabend, S. Ploeger S, *Eur. J. Morphol.*, **31**(4), 290 (1993).
16. E. Calabro, S. Magazu, *Spectroscopy letters: An international Journal of Rapid Communication*, **46**(8), 583 (2013).
17. Calabro, S. Magazu, *Spectroscopy letters: An international Journal of Rapid Communication*, **47**(8), 649 (2014).
18. J. L. Arrondo, M. G. Felix, *Progress in Biophys. and Molecular Biol.*, **72**, 367 (1999).
19. J. L. Arrondo, A. Muga, J. Castresana, F. M. Goni, *Prog. Biophys. Mol. Biol.*, **59**, 23 (1993).
20. C. Polk, E. Postow, CRC Handbook of biological effects of electromagnetic fields, CRC Press, Inc, 1996.
21. N. Radicheva, K. Mileva, T. Vukova, B. Georgieva, I. Kristev, *Arch of Physiol and Biochem*, **110**(3), 203 (2002).
22. J. A. Laurence, P. W. French, R. A. Lindner, D. R. McKenzie, *J. Theor. Biol.*, **206**, 291 (2000).
23. J. A. Laurence, D. R. McKenzie, K. R. Foster, *J. Theor. Biol.*, **222**, 403 (2003).
24. H. Böhr, J. Böhr, *Bioelectromagnetics*, **21**, 68 (2000a).
25. H. Böhr, J. Böhr, *Phys Rev*, **E61**, 312 (2000b).
26. R. D. Astumian, *Phys. Rev. Lett.*, **11**, 118202 (2003).
27. J. Neumann, K. E. Gottschalk, R. D. Astumian, *ACS Nano*, **6**(6), 5242 (2012).
28. H. Fröhlich, *Adv. Electr. And Electr. Phys.*, **53**, 85 (1980).
29. N. N. Neshev, E. I. Kirilova, *Rev. Environ. Health*, **11**, 85 (1996).
30. S. K. Chattopadhyay, K. A. Toews, S. Butt, R. Barlett, H. D. Brown, *Cancer Biochem. Biophys*., **15**, 245 (1997).
31. D. E. Koshland, *Nature medicine*, **4**(10), 1112 (1998).
32. C. J. Thompson, Y. S. Yang, V. Anderson, A. W. Wood, *Bioelectromagnetics*, **21**, 455 (2000).
33. A. Batanov, A. Volkov, V. M. Govorun, A. I. Demin, A. B. Kapitanov, S. V. Timofeev, V. B. Fleurov, Preprint IOFAN (Institute of general physics, Moscow), 3: (in Russian), 1989.
34. H. Frauenfelder, S. G. Sligar, P. G. Wolynes, *Science*, **254**, 1598 (1991).
35. T. Vukova, A. Atanassov, R. Ivanov, N. Radicheva, *MSM*, **11**(2), BR50 (2005).
36. H. Fröhlich, Biological coherence and response to external stimuli, Berlin, Springer-Verlag, 1988, p. 265.
37. H. Fröhlich H, *Proceedings of the Natural Academic Sciences of the USA*, **72**, 4211 (1975).

ПРОМЕНИ В БЕЛТЪЧНАТА КОНФОРМАЦИЯ НА ОБЩ БЕЛТЪК ОТ ЖАБЕШКИ СКЕЛЕТЕН МУСКУЛ СЛЕД ОБЛЪЧВАНЕ С 2.45 GHZ ЕЛЕКТРОМАГНИТНО ПОЛЕ, В ЗАВИСИМОСТ ОТ ИНТЕНЗИТЕТА НА ПОЛЕТО И ОТ ПОГЪЛНАТАТА МОЩНОСТ

Т. И. Апостолова*

Секция „Възбудими Структури, Институт по Биофизика и Биомедицинско инженерство, Българска Академия на Науките, София, България

Постъпила декември, 2014 г.; приета януари, 2015 г.

(Резюме)

Беше направено проучване върху влиянието на електромагнитно поле с честота 2.45 GHz и два интензитета – висок (20 mW/cm^2) и нисък (10 mW/cm^2) съответно. Две различни фракции (центрофугирани на 900 и на 9000 g съответно) бяха подложени на облъчване а другите бяха оставени като контрола (необлъчени) върху лед. По-късно същите фракции бяха лиофилизирани и подложени на инфрачервена спектроскопия. Беше изчислена погълнатата мощност (specific absorption rate, SAR) за двете фракции, облъчени с полета и с двете мощности. Пикът, отговарящ за наличието на вода в лиофилизатите беше премахнат математически. Бяха изчислени площите под характеристичните пикове и рамена, намиращи се в АмидI и АмидII ивиците (характеристични за вторичните белтъчни структури). Наблюдавано беше процентно намаление на α-спиралите и при двете фракции, облъчени с полета и с двата интензитета. Наблюдаваните промени на β–листовете, паралелните β-структури, огъванията и неподредените структури бяха зависими от интензитета на полето и от SAR. Смятаме, че промените във вторичната белтъчна структура са специфични (нетемпературни), тъй като през цялото време се работеше при контролирани температурни условия.